mathematics

MDPI

Article

Enhancing IoT Connectivity in Massive MIMO Networks through Systematic Scheduling and Power Control Strategies

Byung Moo Lee

Department of Intelligent Mechatronics Engineering and Convergence Engineering for Intelligent Drone, Sejong University, Seoul 05006, Republic of Korea; blee@sejong.ac.kr

Abstract: Massive MIMO systems can support a large number of Internet of Things (IoT) devices, even if the number of IoT devices exceeds the number of service antennas in a single base station (BS) located at the data center. In order to improve the performance of Massive MIMO with massive IoT connectivity in a BS, simple scheduling and power control schemes can be of great help, but typically, they require high power consumption in the situation of serious shadow fading. In this paper, we try to improve the performance of Massive MIMO with massive IoT connectivity by using the dropping technique that drops the IoT devices that require high power consumption. Several scheduling and power control schemes have been proposed to increase the spectral efficiency (SE) and the energy efficiency (EE) of Massive MIMO systems. By the combination of these schemes with the dropping technique, we show that the performance can be even further increased under some circumstances. There is a dropping coefficient factor (DCF) to determine the IoT devices that should be dropped. This technique gives more benefits to the power control schemes that require higher power consumption. Simulation results and relevant analyses are provided to verify the effectiveness of the proposed technique.

Keywords: massive connectivity; Internet of Things; energy efficiency; Massive MIMO; scheduling

MSC: 94A05

Citation: Lee, B.M. Enhancing IoT Connectivity in Massive MIMO Networks through Systematic Scheduling and Power Control Strategies. *Mathematics* **2023**, *11*, 3012. https://doi.org/10.3390/math11133012

Academic Editor: Daniel-Ioan Curiac

Received: 13 June 2023
Accepted: 4 July 2023
Published: 6 July 2023

1. Introduction

Recently, it has been shown that Massive multiple-input multiple-output (MIMO) is a highly effective method to enable massive Internet of Things (IoT) networks [1–7]. In order to efficiently accommodate a large number of IoT devices simultaneously based on Massive MIMO systems, a reference signal (RS) can be heavily reused with maximum ratio (MR) processing, and this scheme can provide a moderate data rate with very low power consumption [3,6]. The RS reuse scheme for Massive MIMO with massive IoT connectivity is quite effective for low latency because it does not use any scheduling schemes. However, it has also been shown that some simple scheduling with a power control scheme can increase the system's performance, especially the fairness of spectral efficiency (SE) and energy efficiency (EE) [6–13].

Several other power control and scheduling schemes for Massive MIMO have been proposed. In [14], the authors developed a new model adapting the concept of compatible sets to Massive MIMO, which allows for the efficient solution of a variety of types of optimization problems. They applied their model to the case of joint device scheduling and power control for maximum throughput. In [15], a reference signal (RS) reuse scheme was applied to a device-to-device (D2D) underlaid Massive MIMO system. They made several D2D pairs that were far from each other so they used the same RS, and showed that the effect of RS contamination was greatly decreased by the proposed RS scheduling algorithm. In [16], the authors showed that different fractional power control factors for different processing at the receiver significantly increased the per-user rate. In [17], the authors

determined the number of user equipment (UEs) to be scheduled to maximize SE for a given number of service antennas, and showed various related analyses to improve the performance. With respect to these, the dropping technique, which drops unfavorable UEs, has been extensively applied in several works. Hong et al. proposed it under the line-of-sight (LoS) channel to drop a small number of high-correlation users from the service [18]. In [19], the authors proposed a dropping algorithm to reduce the correlation of the channel with the Tomlinson–Harashima precoder using max–min and equally received power control.

Generally, power control schemes increase SE fairness. However, it requires high power consumption for the UEs that are in bad channel condition. Several important power control and scheduling schemes have been proposed in [6], and it has been shown that by adjusting two inherent parameters in adjustable power control (APC) and adjustable scaled power control (ASPC) schemes, we can obtain any kind of intermediate performance. As well as the high power consumption, the limitation of these schemes is that in the situation of a power-limited case, which means the maximum allowable power consumption is limited, all the IoT devices could fall into bad performance. This is an undesirable situation but usually happens if a Massive-MIMO-based data center is serviced over massive IoT connectivity with serious shadow fading. In this regard, we propose the combination of power control and scheduling with the dropping technique to achieve satisfactory performance even though the IoT devices are under a serious shadow fading situation. Here, the dropping technique refers to the process of disconnecting UE that has undesirable channel conditions. The dropping criterion is decided based on how much more power is required compared to the pre-determined reference power. The power control and scheduling schemes we use in this paper are generalized power control (GPC), scaled power control (SPC), adjustable power control (APC), and adjustable scaled power control (ASPC) [6]. The GPC and APC schemes are applied without considering power consumption, while SPC and ASPC are applied based on the pre-defined power consumption threshold. For this reason, generally, GPC and APC require more power than SPC and ASPC.

The main contributions of this paper are summarized as follows.

- We show that in the case of serious shadow fading, even though there are many good power control and scheduling schemes with adjustable parameters, it is very difficult to achieve the desirable performance. In many algorithms, the adjustable parameters are effective under a given power consumption criterion, and even though we adjust the parameters, the performance can be below the threshold. This is the main limitation of many good schemes with inherent adjustable parameters that can manipulate the performance, and it is necessary to combine other techniques with the schemes.
- Next, based on the motivation and analysis, we combine the dropping technique with several scheduling and power control schemes to improve the performance of Massive MIMO over massive IoT connectivity with the serious shadow fading situation. Under the serious shadow fading situation, a lot of power consumption is required for power control, and it can reduce the performance of the whole system.
- We provide a comprehensive numerical analysis of many good power control and scheduling schemes with the dropping technique under a serious shadow fading environment. We show that the dropping scheme is more effective in the cases of GPC and APC. The performance improvement under SPC and ASPC is marginal, but it can also improve the performance significantly in some situations even though we use scaling schemes such as SPC and ASPC. These analyses can greatly help the system's design and operation.

In what follows, the system model is described in Section 2. In Section 3, we propose the scheduling and power control schemes of RS-reused Massive MIMO with the dropping technique. The dropping technique is extensively applied to the GPC, SPC, APC, and ASPC schemes. Numerical results for the verification of the proposed technique are provided in

Section 4, and concluding remarks are given in Section 5. In addition, we provide the list of abbreviations in Abbreviations.

Notation: Throughout this paper, boldface letters represent vectors and matrices. Boldface lowercase letters represent vectors, and boldface uppercase letters represent matrices. The operators $(\cdot)^{\dagger}$, $(\cdot)^{*}$, $(\cdot)^{T}$, $\mathbb{E}[\cdot]$, and $\mathbb{V}(\cdot)$ signify matrix conjugate transpose, matrix (untransposed) conjugate, matrix transpose, expectation, and variance, respectively. The $M \times M$ identity matrix is denoted by $\mathbf{I}_M$, and $\log_2(\cdot)$ represents the logarithm function with base 2. Additionally, $\mathbf{x} \sim \mathbb{CN}(\mathbf{0}_N, \mathbf{V}_N)$ denotes the complex Gaussian distributed vector with zero mean and covariance $\mathbf{V}_N$. Furthermore, $\mathbb{R}_+$ denotes the set of all positive real numbers, and $\mathbb{R}_{0+} = \{0\} \cup \mathbb{R}_+$. The notation $\mathbb{R}_+^n$, $\mathbb{R}_{0+}^n$, $\mathbb{R}_+^{m\times n}$, and $\mathbb{R}_{0+}^{m\times n}$ refer to the corresponding n-dimensional and $(m \times n)$-dimensional product spaces. If $\mathbb{R}$ is replaced with $\mathbb{C}$, then the corresponding complex spaces are denoted. $\| \cdot \|_\infty$ and $\| \cdot \|_2$ denote l_∞-norm and l_2-norm of vector, respectively.

2. System Model

Considering the uplink Massive MIMO system located at a data center, we assume the number of service antennas at BS is M and the number of IoT devices or UEs is K. Since we assume the situation of massive connectivity of IoT devices, K is much larger than M.

Let

$$\mathbf{G} = [\mathbf{g}_1 \ \cdots \ \mathbf{g}_K] \in \mathbb{C}^{M\times K}, \tag{1}$$

be the $M \times K$ channel matrix between the M-antenna array at the BS based on Massive MIMO and the K active IoT devices or UEs. The channel vector between the k-th UE and the M-antenna array is modeled as,

$$\mathbf{g}_k = \sqrt{\beta_k}\mathbf{h}_k, \quad k = 1, \cdots, K \tag{2}$$

where β_k is the large-scale fading coefficient, and $\mathbf{h}_k$ is the small-scale fading coefficient, respectively.

Alternatively, the matrix $\mathbf{G}$ can be represented in a different form, denoted as follows,

$$\mathbf{G} = \mathbf{H} \cdot \mathrm{diag}\left(\beta_1^{1/2}, \cdots, \beta_K^{1/2}\right), \tag{3}$$

where $\mathbf{H} = [\mathbf{h}_1, \cdots, \mathbf{h}_K] \in \mathbb{C}^{M\times K}$ represents the small-scale fading matrix, and diag$[\cdot]$ denotes the creation of a diagonal matrix. We assume that the IoT devices are uniformly distributed. In addition, we assume that the channel is rich scattering and that the elements of the channel vector $\mathbf{h}_k$ are independent and identically distributed (i.i.d.) and Rayleigh distributed.

The uplink received signal vector can be modeled as

$$\mathbf{y}_\mathrm{u} = \sqrt{p_u}\mathbf{G}\mathbf{x}_\mathrm{u} + \mathbf{n}_\mathrm{u}, \tag{4}$$

where $\mathbf{y}_\mathrm{u} \in \mathbb{C}^M$ is the received signal vector at the M-antenna ports in BS, p_u is the uplink transmission power of each device, $\mathbf{x}_\mathrm{u} \in \mathbb{C}^K$ is the message signal with the power control coefficient from the UE, and $\mathbf{n}_\mathrm{u}$ is the uplink additive white Gaussian noise (AWGN) vector with zero mean and variance σ_{UL}^2 (i.e, $\mathbf{n}_\mathrm{u} \in \mathbb{CN}(\mathbf{0}_M, \sigma_{\mathrm{UL}}^2\mathbf{I}_M)$). The uplink power constraint of the message signal is specified as

$$\|\mathbb{E}[\mathbf{x}_\mathrm{u}^* \odot \mathbf{x}_\mathrm{u}]\|_\infty \leq 1, \tag{5}$$

where $\odot$ denotes the element-wise multiplication.

If we assume $\mathbf{q}_\mathrm{u}$ is the uplink signal with the message before the power control, the relationship between $\mathbf{q}_\mathrm{u}$ and $\mathbf{x}_\mathrm{u}$ can be represented as

$$\mathbf{x}_\mathrm{u} = \mathbf{D}_\eta^{1/2}\mathbf{q}_\mathrm{u}, \tag{6}$$

Here we assume $\mathbf{D}_{\eta}^{1/2} \triangleq \text{diag}\left(\eta_1^{1/2}, \cdots, \eta_K^{1/2}\right)$ is the diagonal matrix, which is used for the power control by the multiplication of $\mathbf{q}_{\text{u}}$. $\boldsymbol{\eta} = [\eta_1 \quad \cdots \quad \eta_K]^{\text{T}}$ is the uplink power control vector, and it satisfies a constraint given to power as follows,

$$\boldsymbol{\eta} \in \mathbb{R}_{+}^{K} \text{ and } \|\boldsymbol{\eta}\|_{\infty} \leq 1. \tag{7}$$

We should apply uplink processing schemes to reduce inter-user interference (IUI), and maximum ratio (MR) processing and zero-forcing (ZF) processing schemes are two well-known and effective schemes for the purpose [20]. It has already been shown that in the situation of a huge amount of IoT devices, which have much greater K than M, ZF processing gives a very low quality of performance, while MR processing gives much better performance [3]. For this reason, for the detection of the uplink signal, we choose MR processing.

The processing matrix $\hat{\mathbf{G}}^{\dagger}$ is used for MR processing where $\hat{\mathbf{G}}$ is the estimate of $\mathbf{G}$. From Equation (4), $\hat{\mathbf{G}}^{\dagger}$ is multiplied to the uplink signal.

$$\hat{\mathbf{G}}^{\dagger}\mathbf{y}_{\text{u}} = \sqrt{p_u}\hat{\mathbf{G}}^{\dagger}\mathbf{G}\mathbf{x}_{\text{u}} + \hat{\mathbf{G}}^{\dagger}\mathbf{n}_{\text{u}}, \tag{8}$$

This paper employs the linear minimum mean square error (LMMSE) channel estimation technique. LMMSE channel estimation aims to minimize the discrepancy between the estimated channel and the actual measured channel. Considering that $\mathbf{h}_k$ follows a Rayleigh distribution, the standard approach is utilized for conducting LMMSE channel estimation.

Time division duplexing (TDD) mode is an effective mode to reduce the RS overhead because uplink channel information can be used for downlink transmission. For this reason, TDD mode is generally applied for Massive MIMO to reduce RS overhead. If we assume each coherence interval lasts τ_c resource elements, we can consider τ_p resource elements are used for the uplink RSs and the remaining $\tau_c - \tau_p$ resource elements are used for uplink data transfer within each coherence interval. Thus, the overhead for transferring uplink RS can be τ_p/τ_c. Based on this fact, the uplink SE can be represented as

$$\mathsf{SE}^{\mathtt{UL}} = \sum_{i=1}^{\kappa^{\text{u}}} \zeta^{\text{u}} \left(1 - \frac{\tau_p}{\tau_c}\right) \log_2(1 + \mathsf{SINR}_i^{\mathtt{UL}}). \tag{9}$$

where $\mathsf{SINR}_{\text{i}}^{\mathtt{UL}}$ is the uplink signal-to-interference and noise ratio (SINR) for ith IoT devices. Let κ^{u} denote the number of coincidentally supported UEs for uplink transmission, while K represents an upper limit on the number of UEs that can be simultaneously supported. It is important to note that κ^{u} is always smaller than K. Since TDD includes both uplink and downlink data, we need to choose a parameter to reflect the amount of uplink and downlink data. If we assume ζ^{u} is the parameter to represent the amount of data transmission resource elements for uplink, and ζ^{d} is the parameter to represent the amount of data transmission resource elements for downlink, we can say that the summation of ζ^{u} and ζ^{d} is one, i.e., $\zeta^{\text{u}} + \zeta^{\text{d}} = 1$.

Assuming $\varsigma^{\text{u}} = \varsigma^{\text{d}} = 0.5$, the uplink throughput (TP) per each UE for ith UE can be,

$$\mathsf{TP}_i = 0.5\mathsf{BW}\left(1 - \frac{\tau_p}{\tau_c}\right) \log_2(1 + \mathsf{SINR}_{\text{i}}^{\mathtt{UL}}). \tag{10}$$

where BW is the system bandwidth. The total TP can be the summation of TP_i for all corresponding i.

In order to accommodate a large number of UEs concurrently, the RS is extensively reused. To represent the RS reuse situation, it is convenient to use the double script notation (j, l) to identify the distributed UEs. We assume $\beta_{j,l}$ is the large-scale fading coefficient between the jth IoT device in the lth group and the BS service antenna array. Then we can arrange all the UEs and corresponding large-scale fading coefficients in a $J \times L$ matrix. In this situation, each column of UEs uses the mutually orthogonal RSs, and we assume

they are in the same group. Each row of UEs uses the same RSs and they are in different group. Therefore, we can represent the large-scale fading matrix as follows.

$$\mathbf{B} = \begin{pmatrix} \beta_{1,1} & \beta_{1,2} & \cdots & \beta_{1,L} \\ \beta_{2,1} & \beta_{2,2} & \cdots & \beta_{2,L} \\ \vdots & \vdots & \vdots & \vdots \\ \beta_{J,1} & \beta_{J,2} & \cdots & \beta_{J,L} \end{pmatrix}, \tag{11}$$

Based on this, with RS reuse and MR processing, we can represent the uplink SINR as follows [3,21].

$$\mathsf{SINR}_{j,l}^{\mathtt{MR},\mathtt{UL}} = \frac{M p_u \gamma_{j,l} \beta_{j,l} \eta_{j,l}}{\sigma_{\mathsf{UL}}^2 + p_u \sum\limits_{j'=1}^{J} \sum\limits_{l'=1}^{L} \beta_{j',l'} \eta_{j',l'} + M p_u \sum\limits_{\substack{l'=1 \\ l' \neq l}}^{L} \gamma_{j,l'} \beta_{j,l'} \eta_{j,l'}}, \tag{12}$$

Next, let us consider the EE metric based on Equation (9). EE is generally defined as rate over the consumption of power. If we assume $P_{\mathsf{PA}}^{\mathtt{UL}}$ is the uplink power amplifier (PA) power consumption and $P_{\mathsf{C}}^{\mathtt{UL}}$ is the rest of power consumption [22], the consumption of sum power can be represented as: $K\left(P_{\mathsf{PA}}^{\mathtt{UL}} + P_{\mathsf{C}}^{\mathtt{UL}}\right) = P_{\mathsf{SUM}}$. The relation between P_{PA} and p_u is $p_u = \mu P_{\mathsf{PA}}$ where μ is the uplink power efficiency of PA.

Then, uplink EE can be shown as

$$\mathsf{EE}^{\mathtt{UL}} = \frac{\sum\limits_{i=1}^{\kappa^{\mathrm{u}}} \zeta^{\mathrm{u}} \left(1 - \frac{\tau_p}{\tau_c}\right) \mathsf{BW} \log_2\left(1 + \mathsf{SINR}_i^{\mathtt{UL}}\right)}{K\left(P_{\mathsf{PA}}^{\mathtt{UL}} + P_{\mathsf{C}}^{\mathtt{UL}}\right)}, \tag{13}$$

where BW represents the system bandwidth.

Fairness is another important metric for supporting numerous IoT devices. SE fairness can be significantly improved using power control [3]. However, it is also known that the EE fairness could be seriously reduced due to the power control. As a fairness metric, Jain's fairness index is generally used [23].

$$\mathcal{F}(\mathsf{SE}) = \frac{\left(\sum\limits_{i=1}^{K} \mathsf{SE}_i\right)^2}{K \sum\limits_{i=1}^{K} \mathsf{SE}_i^2}, \tag{14}$$

$$\mathcal{F}(\mathsf{EE}) = \frac{\left(\sum\limits_{i=1}^{K} \mathsf{EE}_i\right)^2}{K \sum\limits_{i=1}^{K} \mathsf{EE}_i^2}, \tag{15}$$

where SE_i and EE_i are SE and EE of ith IoT devices.

3. RS-Reused Massive MIMO with Dropping Technique

In this section, we show the dropping technique that can be applied to scheduling and power control schemes of Massive MIMO with RS reuse. Several elegant schemes are proposed to improve the performance of Massive MIMO with RS reuse [6,24]. The first scheme is ordering (O), which simply orders the UEs according to the large-scale fading coefficient of each UE. In this case, UE in good channel condition can be paired with UE in bad channel condition for RS reuse, and it increases the SE and EE with the sacrifice of their fairness, $\mathcal{F}(\mathsf{SE})$ and $\mathcal{F}(\mathsf{EE})$. It has also been shown that ascending and descending orders give almost the same performance [6]. The next scheme is GPC. This scheme is widely used, and it uses the ratio of the average large-scale fading coefficient, β_{ave}, and the

corresponding large-scale fading coefficient of ith UE, β_i, to determine the power control coefficient for ith UE, η_i. GPC can maintain very high SE fairness, but the disadvantage of GPC is that it also requires a very high consumption of power, especially under serious shadow fading. To cope with this problem, the SPC scheme is proposed, and this scheme uses the same procedure with GPC maintaining a pre-defined power consumption. Thus, based on the pre-defined power consumption, SPC uses the same power consumption with O and/or Random, which use the pre-defined fixed power consumption. Here, Random is the case of randomly distributed UE, and it is the condition of not applying any scheduling and power control schemes for the improvement of the performance. Both GPC and SPC show very high SE fairness, but SE and EE are relatively low. It is necessary to find the scheme that can achieve the performances between SPC/GPC and O. For this purpose and to increase the flexibility that can determine any kind of intermediate performances of $\mathcal{F}(\mathsf{EE})/\mathcal{F}(\mathsf{SE})$ and EE/SE, the APC and ASPC schemes have been proposed. There are two adjustable parameters in APC and ASPC. By adjusting the two parameters, we can obtain numerous intermediate performances of EE/SE and $\mathcal{F}(\mathsf{EE})/\mathcal{F}(\mathsf{SE})$. There is a power constraint in ASPC so that it does not exceed the pre-defined threshold, while APC consumes a lot of power for some of the UEs that are under serious channel conditions. APC and ASPC use the sigmoid function to adjust output level. We use the following sigmoid function,

$$\Omega(\chi_i; a, b) = \frac{1}{1 + e^{-a(\chi_i - b)}}, \tag{16}$$

where χ_i is the input, and a, b indicate the parameters to adjust the output of the sigmoid function. a and b can be chosen arbitrarily, and based on these, we can obtain any value for the trade-off between EE and SE, with fairnesses. Figure 1 presents the relationship between input and output based on the variations of a and b in sigmoid function, when χ_i is 0.2, 0.5, and 0.8. The output tends to be high when a is large and b is small.

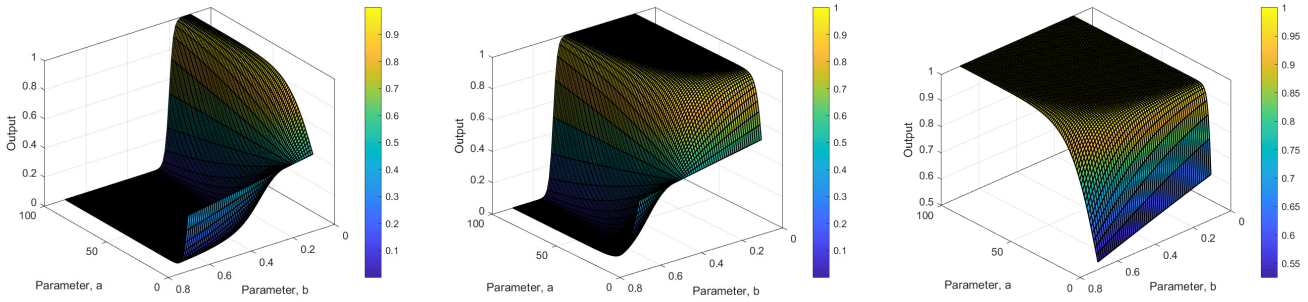

Figure 1. Input and output relations with a and b variations in sigmoid function, when $\chi_i = 0.2$, $\chi_i = 0.5$, and $\chi_i = 0.8$ (from left to right).

The dropping technique is effective, especially if there is serious shadow fading. We provide the simulation results of ASPC under shadow fading in Figure 2. For the simulations, we use coherence time $T_c = 50$ ms, the number of service antennas $M = 400$, and the number of UEs $K = 840$. The detailed simulation parameters are given in the next section. As observed, SE performance is reduced from the location of high a if the standard deviation of shadowing, σ_{shadow}, is increased. There is pre-defined power consumption in ASPC, thus accommodating many IoT devices with high σ_{shadow} results in performance loss.

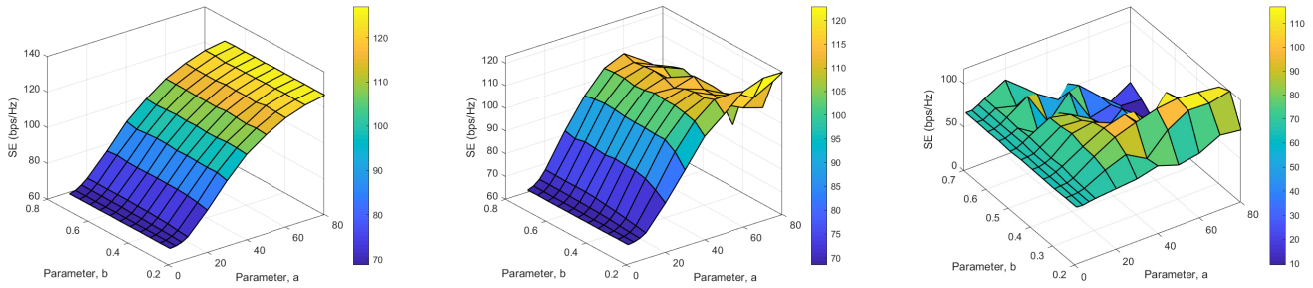

Figure 2. SE performances based on a and b variations in sigmoid function. SE (bps/Hz) versus a and b when $\sigma_{\text{shadow}} = 0$ dB, $\sigma_{\text{shadow}} = 3$ dB, and $\sigma_{\text{shadow}} = 8$ dB (from left to right).

In this situation, disconnecting some of the IoT devices that are in poor channel condition can improve the performance of the network. Determining the dropping threshold is an important issue in this technique. For this, we use the dropping coefficient factor (DCF), $\varepsilon_{\text{drop}}$, for the dropping criterion. If some UEs require more than $\varepsilon_{\text{drop}}$ times power consumption compared to initial power consumption p_u, then we disconnect the corresponding UEs. That is, we drop the UEs that require more power than $\varepsilon_{\text{drop}} \times p_u$. All UEs except the dropped UEs are gathered in G_1.

Now, we can represent the algorithms GPC, SPC, APC, and ASPC with the dropping technique. Algorithm 1 shows GPC with the dropping technique. To determine the power coefficient factor for ith UE, η_i, β_{ave} is divided by β_i (Line 8). If the determined power for ith UE $p_{u,i}$ (Line 10) is smaller than $p_u \times \varepsilon_{\text{drop}}$, it is included in the service group (Line 13). If not, the UE is disconnected. $\varepsilon_{\text{drop}}$ can be determined based on the system requirements. If $\varepsilon_{\text{drop}}$ is too high, no UE would be disconnected, and if $\varepsilon_{\text{drop}}$ is too low, most of the UEs could be disconnected. After that, K_{s}, the number of UEs after dropping is determined (Line 14), and the processing matrix $\mathbf{V}$ is generated based on K_{s} (Line 15). The received signal is multiplied by $\mathbf{V}$ to reduce IUI (Line 16). Then G_1 is emptied, and the same procedure is repeated in the pre-defined number $\Gamma_{\texttt{Len}}$.

Algorithm 1: Generalized Power Control (GPC) with Dropping (GPC(D))

1 Initialization;
2 $G_1 \Leftarrow ; \quad l = 0$;
3 **while** $l \leq \Gamma_{Len}$ **do**
4 Select UEs ;
5 $\beta_{\text{ave}} \leftarrow \frac{\sum_{i=1}^{K} \beta_i}{K}$;
6 Form $\mathbf{B} \in \mathbb{C}^{J \times L}$;
7 **for** $i = 1 : K$ **do**
8 $\eta_i \leftarrow \beta_{\text{ave}} / \beta_i$;
9 Send η_i to UE_i ;
10 $p_{u,i} \leftarrow p_u \cdot \eta_i$;
11 **if** $p_{u,i} < p_u \varepsilon_{drop}$;
12 **then**
13 $G_1 \Leftarrow \{G_1, UE_i\}$;
14 $K_{\text{s}} \Leftarrow \texttt{length}(G_1)$;
15 Generate $\mathbf{V} \in \mathbb{C}^{K_{\text{s}} \times M}$;
16 $\mathbf{y}_{\text{u}} \leftarrow \mathbf{V} \cdot \sqrt{p_u} \mathbf{G} \mathbf{x}_{\text{u}} + \mathbf{n}_{\text{u}}$;
17 $G_1 \Leftarrow ; \quad l = l + 1$;

Algorithm 2 shows SPC with the dropping technique. In SPC, η_i is determined based on the pre-determined threshold, η^{REF} (Line 11). In this paper, we assume total

power allocation is the same as the initially determined total power consumption (Line 13). The same dropping logic as GPC is applied (Line 15 $\sim$ 17). After disconnecting the undesirable UEs, the procedure for the determination of η_i proceeds based on the newly determined number of UEs, K_{s} (Line 19 $\sim$ 29).

Algorithm 2: Scaled Power Control (SPC) with Dropping (SPC(D))

1 Initialization;
2 $G_1 \Leftarrow ; \quad l = 0$;
3 **while** $l \leq \Gamma_{Len}$ **do**
4 Select UEs ;
5 $\beta_{\mathsf{ave}} \leftarrow \frac{\sum_{i=1}^{K} \beta_i}{K}$;
6 Form $\mathbf{B} \in \mathbb{C}^{J \times L}$;
7 $\mathrm{Y} \leftarrow p_u \cdot \beta_{\mathsf{ave}}$;
8 **for** $i = 1 : K$ **do**
9 $\eta_i \leftarrow \beta_{\mathsf{ave}} / \beta_i$;
10 $\eta^{\mathtt{SUM}} \leftarrow \sum_{i=1}^{K} \eta_i$;
11 $\eta^{\mathtt{REF}} \leftarrow p_u \cdot K$;
12 **for** $i = 1 : K$ **do**
13 $\eta_i \leftarrow \left(\frac{\beta_{\mathsf{ave}}}{\beta_i}\right) \cdot \left(\frac{\eta^{\mathtt{REF}}}{\eta^{\mathtt{SUM}}}\right)$;
14 $p_{u,i} \leftarrow p_u \cdot \eta_i$;
15 **if** $p_{u,i} < p_u \varepsilon_{drop}$;
16 **then**
17 $G_1 \Leftarrow \{G_1, UE_i\}$;
18 $K_{\mathsf{s}} \Leftarrow \mathtt{length}(G_1)$;
19 $\beta_{\mathsf{ave}} \leftarrow \frac{\sum_{i=1}^{K_{\mathsf{s}}} \beta_i}{K_{\mathsf{s}}}$;
20 Form $\mathbf{B} \in \mathbb{C}^{J_{\mathsf{s}} \times L}$;
21 $\mathrm{Y} \leftarrow p_u \cdot \beta_{\mathsf{ave}}$;
22 **for** $i = 1 : K_{\mathsf{s}}$ **do**
23 $\eta_i \leftarrow \beta_{\mathsf{ave}} / \beta_i$;
24 $\eta^{\mathtt{SUM}} \leftarrow \sum_{i=1}^{K_{\mathsf{s}}} \eta_i$;
25 $\eta^{\mathtt{REF}} \leftarrow p_u \cdot K_{\mathsf{s}}$;
26 **for** $i = 1 : K_{\mathsf{s}}$ **do**
27 $\eta_i \leftarrow \left(\frac{\beta_{\mathsf{ave}}}{\beta_i}\right) \cdot \left(\frac{\eta^{\mathtt{REF}}}{\eta^{\mathtt{SUM}}}\right)$;
28 Send η_i to UE_i ;
29 $p_{u,i} \leftarrow p_u \cdot \eta_i$;
30 Generate $\mathbf{V} \in \mathbb{C}^{K_{\mathsf{s}} \times M}$;
31 $\mathbf{y}_{\mathrm{u}} \leftarrow \mathbf{V} \cdot \sqrt{p_u} \mathbf{G} \mathbf{x}_{\mathrm{u}} + \mathbf{n}_{\mathrm{u}}$;
32 $G_1 \Leftarrow ; \quad l = l + 1$;

Algorithms 3 and 4 present APC and ASPC with the dropping technique, respectively. They also use the same dropping logic that drops the UEs that require higher power than the threshold. There are two inherent parameters a and b, and based on the parameters, K_{s} can be significantly different.

Algorithm 3: Adjusted Power Control (APC) with Dropping (APC(D))

Initialization;
$G_1 \Leftarrow ; \quad l = 0$;
while $l \leq \Gamma_{Len}$ **do**
  Select UEs ;
  Determine a and b ;
  $\beta_{\mathsf{ave}} \leftarrow \frac{\sum_{i=1}^{K} \beta_i}{K}$;
  Form $\mathbf{B}(:) \in \mathbb{C}^{K \times 1}$;
  $\mathbf{B}_{\mathtt{sort}}(:) \leftarrow \mathsf{sort}(\mathbf{B}(:), \Xi_i)$;
  for $i = 1 : K$ **do**
    $\mathsf{PL}_i \leftarrow 10 \log_{10}\left(\frac{1}{\beta_i}\right)$;
  for $i = 1 : K$ **do**
    if $\Xi_i == \Xi_1$ **then**
      $\chi_i \leftarrow \frac{\mathsf{PL}_i - \mathsf{PL}_1}{\mathsf{PL}_K}$;
    else if $\Xi_i == \Xi_2$ **then**
      $\chi_i \leftarrow \frac{\mathsf{PL}_i - \mathsf{PL}_K}{\mathsf{PL}_1}$;
    $\Omega_i(\chi_i; a, b) \leftarrow \frac{1}{1+e^{-a(\chi_i - b)}}$;
    $\eta_i \leftarrow \left(\frac{\beta_{\mathsf{ave}}}{\beta_i}\right) \Omega_i(\chi_i; a, b)$;
    Send η_i to UE_i ;
    $p_{u,i} \leftarrow p_u \cdot \eta_i$;
    if $p_{u,i} < p_u \varepsilon_s$;
    then
      $G_1 \Leftarrow \{G_1, UE_i\}$;
  $K_{\mathsf{s}} \Leftarrow \mathtt{length}(G_1)$;
  $\mathbf{B} \leftarrow \mathsf{reshape}(\mathbf{B}_{\mathtt{sort}}(:), J_{\mathsf{s}}, L)$;
  Generate $\mathbf{V} \in \mathbb{C}^{K_{\mathsf{s}} \times M}$;
  $\mathbf{y}_{\mathrm{u}} \leftarrow \mathbf{V} \cdot \sqrt{p_u} \mathbf{G} \mathbf{x}_{\mathrm{u}} + \mathbf{n}_{\mathrm{u}}$;
  $G_1 \Leftarrow ; \quad l = l + 1$;

Algorithm 4: Adjusted Scaled Power Control (ASPC) with Dropping (ASPC(D))

1 Initialization;
2 $G_1 \Leftarrow ; \quad l = 0$;
3 **while** $l \leq \Gamma_{Len}$ **do**
4 Select UEs ;
5 Determine a and b ;
6 $\beta_{\mathsf{ave}} \leftarrow \frac{\sum_{i=1}^{K} \beta_i}{K}$;
7 Form $\mathbf{B}(:) \in \mathbb{C}^{K \times 1}$;
8 $\mathbf{B}_{\mathtt{sort}}(:) \leftarrow \mathsf{sort}(\mathbf{B}(:), \Xi_i)$;
9 **for** $i = 1 : K$ **do**
10 $\mathsf{PL}_i \leftarrow 10 \log_{10}\left(\frac{1}{\beta_i}\right)$;
11 **for** $i = 1 : K$ **do**
12 **if** $\Xi_i == \Xi_1$ **then**
13 $\chi_i \leftarrow \frac{\mathsf{PL}_i - \mathsf{PL}_1}{\mathsf{PL}_K}$;
14 **else if** $\Xi_i == \Xi_2$ **then**
15 $\chi_i \leftarrow \frac{\mathsf{PL}_i - \mathsf{PL}_K}{\mathsf{PL}_1}$;
16 $\Omega_i(\chi_i; a, b) \leftarrow \frac{1}{1+e^{-a(\chi_i - b)}}$;
17 $\eta_i \leftarrow \left(\frac{\beta_{\mathsf{ave}}}{\beta_i}\right) \Omega_i(\chi_i; a, b)$;
18 $B \leftarrow \mathsf{reshape}(B_{\mathtt{sort}}(:), J, L)$;
19 $\eta^{\mathtt{SUM}} \leftarrow \sum_{i=1}^{K} \eta_i$;
20 $\eta^{\mathtt{REF}} \leftarrow \rho_u \cdot K$;
21 **for** $i = 1 : K$ **do**
22 $\eta_i \leftarrow \left(\frac{\beta_{\mathsf{ave}}}{\beta_i}\right) \Omega_i(\chi_i; a, c) \cdot \left(\frac{\eta^{\mathtt{REF}}}{\eta^{\mathtt{SUM}}}\right)$;
23 $p_{u,i} \leftarrow p_u \cdot \eta_i$;
24 **if** $p_{u,i} < p_u \varepsilon_{drop}$;
25 **then**
26 $G_1 \Leftarrow \{G_1, UE_i\}$;
27 $K_{\mathsf{s}} \Leftarrow \mathtt{length}(G_1)$;
28 Repeat Line 6 $\sim$ 20 with K_{s} ;
29 **for** $i = 1 : K_{\mathsf{s}}$ **do**
30 $\eta_i \leftarrow \left(\frac{\beta_{\mathsf{ave}}}{\beta_i}\right) \Omega_i(\chi_i; a, c) \cdot \left(\frac{\eta^{\mathtt{REF}}}{\eta^{\mathtt{SUM}}}\right)$;
31 Send η_i to UE_i ;
32 $p_{u,i} \leftarrow p_u \cdot \eta_i$;
33 $\mathbf{B} \leftarrow \mathsf{reshape}(\mathbf{B}_{\mathtt{sort}}(:), J_{\mathsf{s}}, L)$;
34 Generate $\mathbf{V} \in \mathbb{C}^{K_{\mathsf{s}} \times M}$;
35 $\mathbf{y}_{\mathrm{u}} \leftarrow \mathbf{V} \cdot \sqrt{p_u} \mathbf{G} \mathbf{x}_{\mathrm{u}} + \mathbf{n}_{\mathrm{u}}$;
36 $G_1 \Leftarrow ; \quad l = l + 1$;

4. Numerical Results and Discussion

In this section, we present the numerical analysis and relevant discussion of the dropping technique with various power control and scheduling schemes. We employ Monte Carlo simulations to validate the proposed algorithms.

In our simulation, we assume that the BS is able to measure the strength of the received signal from each UE terminal and estimate the large-scale fading coefficient. We also assume that the BS is able to calculate the power control coefficients and send the information to the corresponding UE terminals. We provide the detailed simulation scenario as follows:

- The simulation is conducted in a 2D environment with a single BS and multiple UEs.

- The BS is located at the origin of the coordinate system, and the UE terminals are randomly distributed within a circular area with radius $R = 750$ m.
- The channel between the BS and each UE terminal is assumed to be a Rayleigh fading channel.
- The UE terminals are assumed to use a power control algorithm to adjust their transmit power in order to improve performance.

The power control procedures are assumed and implemented as follows:

1. BS measurement: In our simulation, the BS measures the strength of the RS transmitted by the UEs. Based on these measurements, the BS estimates the large-scale fading coefficient associated with each UE's channel.
2. Power control coefficient calculation: Using the estimated fading coefficients, the BS calculates the power control coefficients that determine the desired power level for each UE. The power control coefficients are determined based on the specific power control algorithm employed in the simulation.
3. Signaling transmission: The BS then communicates the power control coefficients and related information to the corresponding UEs. This signaling is achieved through dedicated signaling channels or control channels, depending on the specific wireless standard or protocol considered in our simulation.
4. UE power adjustment: Upon receiving the signaling information from the BS, each UE adjusts its transmit power level accordingly. The UEs increase or decrease their power based on the power control coefficients provided by the BS, aiming to achieve the desired power levels for optimal performance.

It is postulated that both process (1) and process (3) are executed with optimal precision, devoid of any inherent operational errors.

The simulation parameters that are used in this paper are provided in Table 1. We assume a high-density urban outdoor scenario. The choice of the 180 kHz coherence bandwidth, denoted as B_c, aligns with one resource block of 3GPP systems and is relevant to the specific context of our investigation. By choosing B_c = 180 kHz, we can generate a serious RS reuse situation in a massive IoT scenario. The uplink initial power is the uplink average radiation power.

Table 1. Simulation Parameters.

Parameter	Value
Coherence Time, T_c	5, 50 ms
Coherence Bandwidth, B_c	180 kHz
Portion of data trans. resource elements, ζ^u,ζ^d	0.5
Signal Bandwidth, BW	20 MHz
Uplink initial power, p_u	10 mW
Path Loss Model	ETSI
Antenna Gains of BS and UE, G_{BS}, G_{UE}	0 dB
BS noise figure, NF_{BS}	9 dB
Default Dropping Coefficient Factor (DCF), ε_{s}	10
Standard deviation of shadow fading, σ_{Shadow}	8 dB
RX Processing	MR

We use the Massive MIMO system with $M = 400$ and maximum number of UEs, $K_{max} = 12,000$ using $T_c = 5$ ms and 50 ms. Considering the 3GPP system model that has 14 resource elements in a 15 kHz bandwidth and 1 ms interval, if we assume the coherence bandwidth $B_c = 180$ kHz, there are 840 available resource elements when

$T_c = 5$ ms, and 8400 resource elements when $T_c = 50$ ms. Since we allocate half of the available resource elements to RS, 420 resource elements are available for data transmission when $T_c = 5$ msec, and 4200 resource elements are available for data transmission when $T_c = 50$ ms. The uplink initial power $p_u = 10$mW and the input-back off is 8 dB for the compensation of the PA nonlinearity. We assume the maximum PA efficiency without input-backoff is 50%. The ETSI urban macro path loss model is used [25].

$$\mathsf{PL} = 128.1 + 37.6 \log_{10}(R). \tag{17}$$

Figure 3 shows the performances of the dropping technique based on the cumulative distribution function (CDF). Figure 3a is the probability versus throughput (TP) (Mbps/Hz) when $K = 840$ and $T_c = 5$ ms. In this case, the RS reuse factor is $L = 2$. Here, the scheme "(D)" indicates the scheme with the dropping technique. As observed, the GPC and APC schemes with the dropping technique give a very high TP improvement. There is also some TP improvement when we use SPC and ASPC with the dropping technique, but the performance improvement is marginal compared to the cases of GPS and APC. In this paper, we use $a = 5$ and $b = 0.5$ for the parameters of APC and ASPC. If we used different parameters, the performance improvement would be different. Figure 3b,c show the probability versus TP (Mbps) when $K = 8400$ with $T_c = 5$ ms and 50 ms, respectively. When $T_c = 5$ ms, L becomes 20. Due to the serious interference, the performance improvement is reduced. When $T_c = 50$ ms, L is still 2, and thus it shows a very similar characteristic with the case of $K = 840$ and $T_c = 5$ msec. Figure 3d–f present the cases of probability versus EE (Mbps/Hz). GPC and APC with the dropping technique still give very high EE performance improvements.

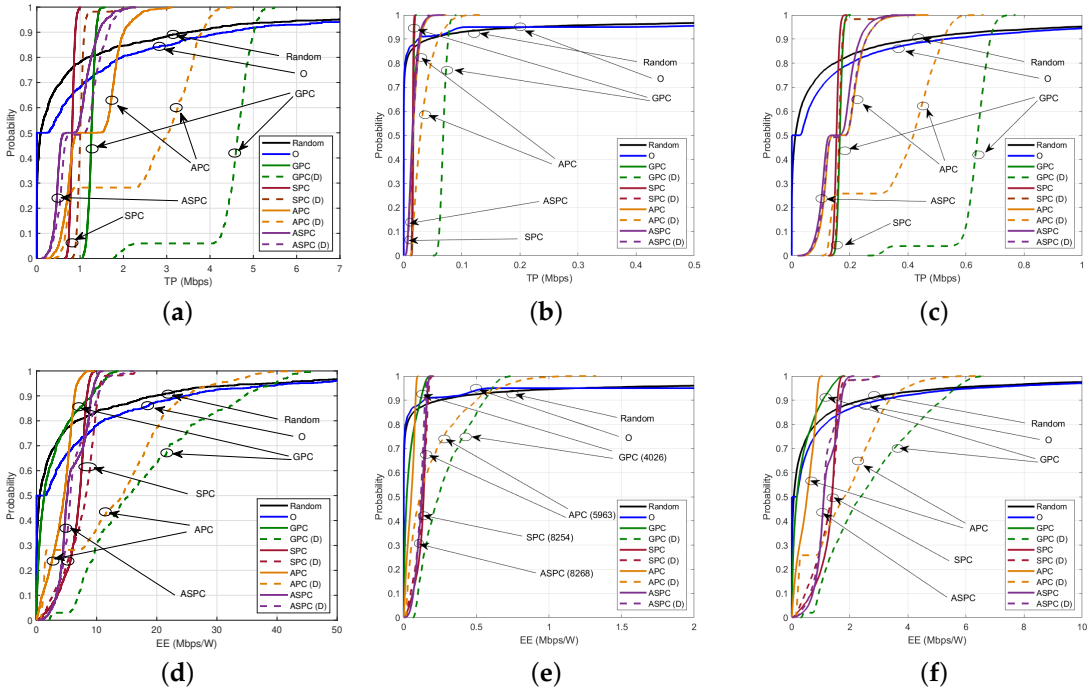

Figure 3. Performances of dropping technique based on cumulative distribution function (CDF). (**a**) Probability versus TP (throughput) (Mbps) when $K = 840$ and $T_c = 5$ ms. (**b**) Probability versus TP (Mbps) when $K = 8400$ and $T_c = 5$ ms. (**c**) Probability versus TP (Mbps) when $K = 8400$ and $T_c = 50$ ms. (**d**) Probability versus EE (Mbps/W) when $K = 840$ and $T_c = 5$ ms. (**e**) Probability versus EE (Mbps/W) when $K = 8400$ and $T_c = 5$ ms. (**f**) Probability versus EE (Mbps/W) when $K = 8400$ and $T_c = 50$ ms (from left to right).

Remark 1. *Using the dropping technique, both GPC and APC demonstrate remarkable enhancements in terms of SE and EE performance. On the other hand, although SPC and ASPC with the*

dropping technique also exhibit improved SE and EE performance, the magnitude of the improvements is marginal compared to GPC and APC with the dropping technique. Additionally, as L increases, the degree of improvement decreases.

Figure 4 presents the performances based on various metrics, such as EE, SE, $\mathcal{F}(\mathsf{EE})$, $\mathcal{F}(\mathsf{SE})$, and P_{SUM}. In these figures, we show how the performance metrics change as K increases. Red 'O's indicate simulation results, and we can observe that the simulation results and theoretical analysis match well. Figure 4a,b show the SE versus K when $T_c = 5$ ms and 50 ms, respectively. As observed, the dropping technique moves the SE performance curve to the right, and we can consider using it in the large K to achieve higher performance. Noticeably, we still see that we can obtain a higher performance improvement when we apply the dropping technique to GPC and APC. This is because we use GPC and APC without the constraint of power consumption, while SPC and ASPC have the constraint of power consumption.

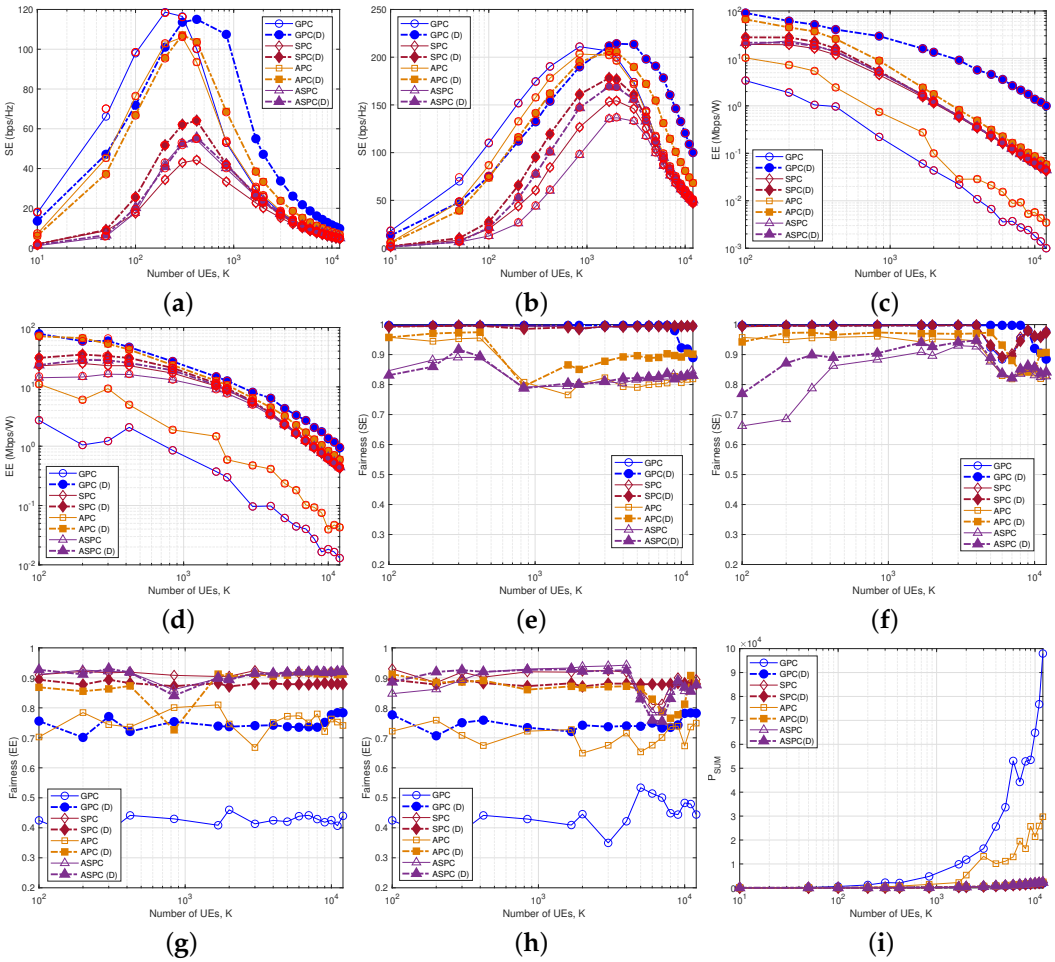

Figure 4. SE, EE, and fairness performances: (**a**) SE versus K when $T_c = 5$ ms, (**b**) SE versus K when $T_c = 50$ ms, (**c**) EE versus K when $T_c = 5$ ms, (**d**) EE versus K when $T_c = 50$ ms, (**e**) fairness (SE) versus K when $T_c = 5$ ms, (**f**) fairness (SE) versus K when $T_c = 50$ ms, (**g**) EE versus K when $T_c = 5$ ms, (**h**) fairness (EE) versus K when $T_c = 50$ ms, (**i**) P_{SUM} versus K when $T_c = 50$ ms (from left to right).

Remark 2. *The dropping technique shifts the SE performance curve to the right, and gives higher performance when K is large.*

Figure 4c,d show the EE versus K when $T_c = 5$ ms and 50 ms, respectively. Without the dropping technique, both GPC and APC give very low EE performances. In particular, GPC

presents the lowest EE performances. On the other hand, GPC with the dropping technique gives the highest EE for both cases, and APC with the dropping technique also gives a very high EE performance. This is a very desirable result in that we can improve EE significantly with a simple dropping technique. SPC and ASPC with the dropping technique also show good EE performance improvement, but the performance improvement from the dropping technique is marginal compared to the cases of GPC and APC.

Remark 3. *The utilization of the dropping technique yields the most substantial EE performance improvements in GPC and APC, while the absence of the dropping technique results in the lowest EE performances. The enhancement in EE is particularly noteworthy for GPC and APC.*

Figure 4e,f show the $\mathcal{F}(\mathsf{SE})$ versus K when $T_c = 5$ ms and 50 ms, respectively. In the case of GPC, the dropping technique has little effect on $\mathcal{F}(\mathsf{SE})$. In the case of APC, again the dropping technique does not give any meaningful change in $\mathcal{F}(\mathsf{SE})$.

Remark 4. *GPC and APC with the dropping technique have little effect on $\mathcal{F}(SE)$.*

Figure 4g,h present the $\mathcal{F}(\mathsf{EE})$ versus K when $T_c = 5$ ms and 50 ms, respectively. GPC and APC with the dropping technique significantly improve the $\mathcal{F}(\mathsf{EE})$, and SPC and ASPC with the dropping technique give similar $\mathcal{F}(\mathsf{EE})$ performances to those without the dropping technique.

Remark 5. *Applying the dropping technique to GPC and APC results in a significant enhancement of $\mathcal{F}(EE)$, while having no reduction in $\mathcal{F}(SE)$.*

Figure 4i presents P_{SUM} versus K when $T_c = 5$ ms. As expected, GPC and APC require too much power as K increases, and the dropping technique can significantly reduce the P_{SUM}. When $T_c = 50$ ms, the situation is very similar to the case of $T_c = 5$ ms.

Figure 5 presents the 3D performances based on various parameters when $K = 8400$ and $T_c = 50$ ms. Figure 5a,b show the SE versus DCF, $\varepsilon_{\mathsf{drop}}$ and σ_{shadow} (dB). The performance difference between GPC/APC and SPC/ASPC is high when σ_{shadow} is high. Figures 5c,d show the EE versus DCF and σ_{shadow} (dB). Again, we can observe that the performance difference between GPC/APC and SPC/ASPC is high when σ_{shadow} is high. Figure 5e,f show the $\mathcal{F}(\mathsf{SE})$. For the careful choice of GPC and APC with the dropping technique, they can present better $\mathcal{F}(\mathsf{SE})$ than SPC/ASPC. The case of $\mathcal{F}(\mathsf{EE})$ also presents similar characteristics as shown in Figure 5g,h.

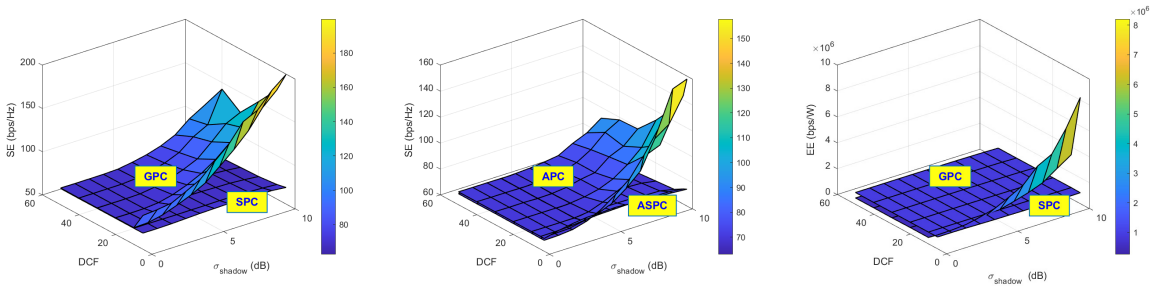

(**a**) (**b**) (**c**)

Figure 5. *Cont.*

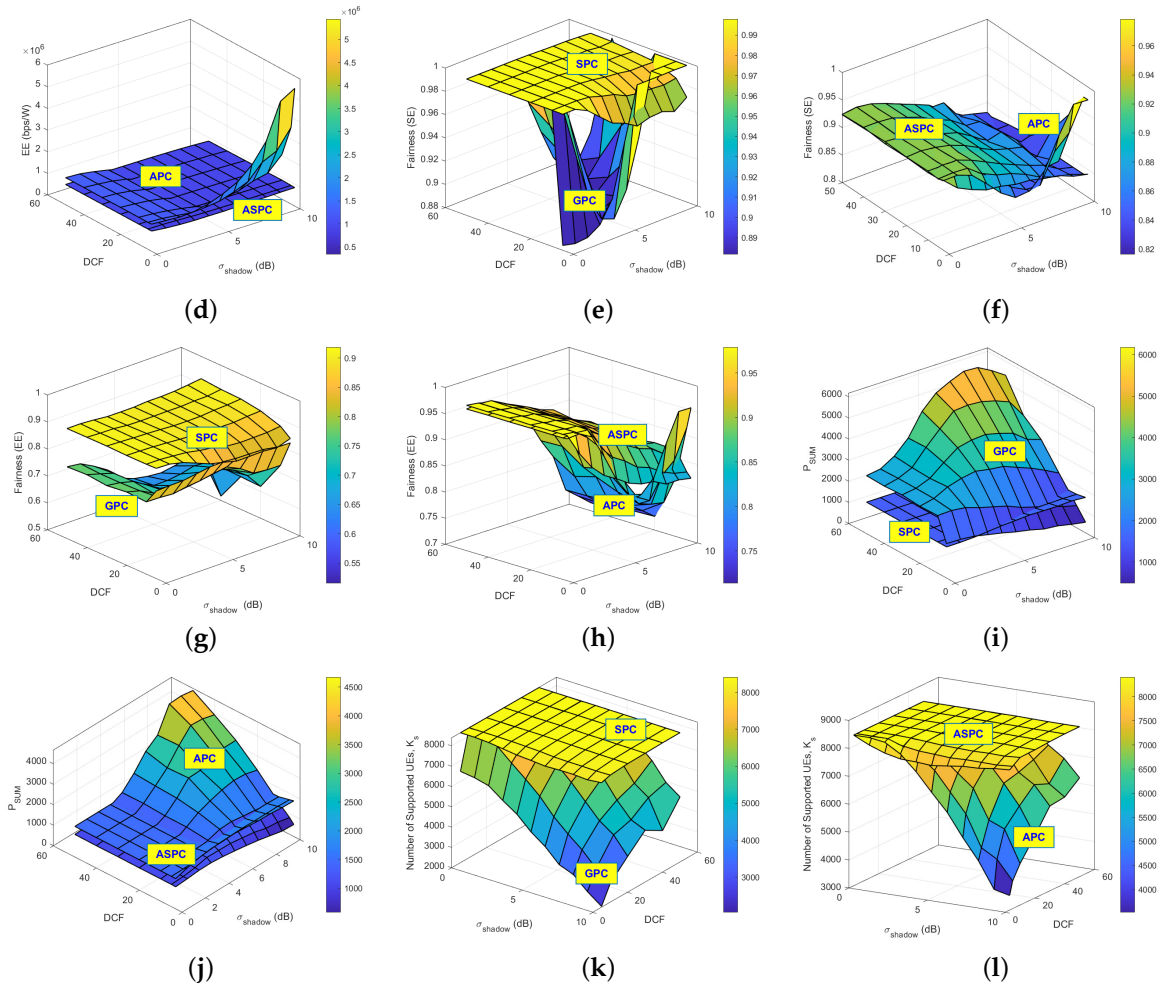

Figure 5. Three-dimensional performances based on various parameters when $K = 8400$ and $T_c = 50$ ms: (**a**) SE(bps/Hz) of GPC and SPC versus DCF and σ_{shadow} (dB), (**b**) SE(bps/Hz) of APC and ASPC versus DCF and σ_{shadow} (dB), (**c**) EE(bps/W) of GPC and SPC versus DCF and σ_{shadow} (dB), (**d**) EE(bps/W) of APC and ASPC versus DCF and σ_{shadow} (dB), (**e**) fairness (SE) of GPC and SPC versus DCF and σ_{shadow} (dB), (**f**) fairness (SE) of APC and ASPC versus DCF and σ_{shadow} (dB), (**g**) fairness (EE) of GPC and SPC versus DCF and σ_{shadow} (dB), (**h**) fairness (EE) of APC and ASPC versus DCF and σ_{shadow} (dB), (**i**) P_{SUM} of GPC and SPC versus DCF and σ_{shadow} (dB), (**j**) P_{SUM} of APC and ASPC versus DCF and σ_{shadow} (dB), (**k**) K_{support} of GPC and SPC versus DCF and σ_{shadow} (dB), (**l**) K_{support} of APC and ASPC versus DCF and σ_{shadow} (dB) (from left to right).

Remark 6. *By selecting the suitable DCF, GPC/APC can achieve superior $\mathcal{F}(SE)$ and $\mathcal{F}(EE)$ performances compared to SPC/ASPC.*

Generally, if DCF is large, GPC and APC consume more power (Figure 5i,j). This is because when DCF is large, GPC and APC support more UEs (Figure 5k,l). Compared with GPC/APC, for the cases of SPC/ASPC, the number of supported UEs does not change so much for the various values of σ_{shadow} and DCF.

Remark 7. *K_s in SPC/ASPC remains relatively unchanged for different values of σ_{shadow} and DCF. Conversely, K_s in GPC/APC experiences significant variation based on the choice of σ_{shadow} and DCF.*

We present the summary for the gains of the dropping technique in Table 2. When we use GPC (D) and APC (D), we can achieve high SE and EE gains. In particular, we

can achieve quite a large amount of EE gain. $\mathcal{F}(\mathsf{SE})$ is maintained even though we apply the dropping technique. We can also increase $\mathcal{F}(\mathsf{EE})$ significantly when we use GPC (D) and APC (D). The amount of power saving is also quite large so that when $T_c = 50$ ms, $K = 3000$, with GPC (D), a gain in P_{SUM} of around 6898% is reached. We can also improve the EE and SE performances of SPC/ASPC using the dropping technique even though the improvements are not so significant when compared to the cases of GPC/APC using the dropping technique.

Table 2. Summary for the gains of dropping technique in numerical values.

Classification		Schemes	SE Gain	EE Gain	$\mathcal{F}$(SE) Gain	$\mathcal{F}$(EE) Gain	P_{SUM} Gain
$T_c = 5$ ms	$K = 840$	GPC (D)	104.06%	13,309.09%	0.16%	77.66%	3641.41%
		SPC (D)	26.42%	20.12%	0.99%	4.13%	4.91%
		APC (D)	28.02%	1103.34%	1.63%	18.63%	845.13%
		ASPC (D)	18.91%	21.0%	0.56%	0.1 %	2.2 %
	$K = 3000$	GPC (D)	32.40%	41,877.12%	0.46%	79.19%	3429.03%
		SPC (D)	10.24%	3.31%	0.14%	4.94%	6.31%
		APC (D)	27.37%	2776.8%	6.67%	19.75%	1226.66%
		ASPC (D)	2.17%	0.12%	1.13%	0.1%	1.2%
$T_c = 50$ ms	$K = 3000$	GPC (D)	22.77%	8326.84%	0%	110.81%	6898.45%
		SPC (D)	9.93%	3.8%	0%	4.98%	5.93%
		APC (D)	10.48%	1263.83%	1.55%	28.97%	1186.07%
		ASPC (D)	17.14%	8.99%	2.21%	1.72%	0.47%
	$K = 8000$	GPC (D)	100.33%	7441.41%	4.54%	63.76%	3713.89%
		SPC (D)	5.37%	1.11%	1.4%	0.58%	6.49%
		APC (D)	33.82%	1295.70%	0.43%	12.22%	974.22%
		ASPC (D)	7.99%	1.55%	1.85%	2.71%	0.27%

The summary of the performances is given in Table 3. In this table, ◎ indicates very good performance, ○ indicates relatively good performance, △ indicates acceptable performance, and × indicates poor performance. We can choose the appropriate scheme based on the possible applications.

Table 3. Summary of performances.

Schemes	SE	EE	$\mathcal{F}$(SE)	$\mathcal{F}$(EE)	P_{SUM}	K_s
GPC	○	×	◎	△	×	◎
GPC (D)	◎	◎	◎	○	○	×
SPC	×	△	◎	◎	○	◎
SPC (D)	×	△	◎	◎	○	○
APC	○	×	○	○	×	◎
APC (D)	○	○	○	○	○	×
ASPC	×	○	○	◎	○	◎
ASPC (D)	×	○	○	◎	○	○

5. Conclusions

In this paper, we have proposed the dropping technique that can be combined with several scheduling and power control schemes in Massive MIMO enabling massive IoT devices. With the appropriate dropping technique, we showed that the performances of Massive MIMO can be significantly improved. The performance metrics we used in this paper were SE, EE, $\mathcal{F}(\mathsf{SE})$, $\mathcal{F}(\mathsf{EE})$, and P_{SUM}. We analyzed both cases of $T_c = 5$ ms and 50 ms. When we combine the dropping technique with the GPC and APC schemes, we can obtain very high SE and EE performance improvements. $\mathcal{F}(\mathsf{EE})$ can also be improved with little performance loss of $\mathcal{F}(\mathsf{SE})$. When we combine the dropping technique with SPC and ASPC, we can still obtain some performance improvement, but the improvement is marginal compared to the cases of GPC and APC. This is because SPC and ASPC have a pre-defined power consumption threshold that must be maintained, and they are already designed to reduce their power consumption and improve the EE. There are many scheduling and power control schemes and many parameters that can be used to adjust the performance. The appropriate choices and combinations of these schemes with the dropping technique can significantly improve many performance metrics. The results in this paper can be a useful design tool for the realization of high-performance Massive MIMO with massive IoT connectivity systems.

Funding: This work was supported by the Basic Science Research Program through the National Research Foundation of Korea (NRF) funded by the Korean government (MSIT) under Grant NRF-2023R1A2C1002656, was supported by the MSIT (Ministry of Science and ICT), Korea, under Grant IITP-2023-RS-2022-00156345 (ICT Challenge and Advanced Network of HRD Program), and was supported by the faculty research fund of Sejong University in 2023.

Data Availability Statement: Not applicable.

Conflicts of Interest: The author declares no conflict of interest.

Abbreviations

APC	Adjustable Power Control
ASPC	Adjustable Scaled Power Control
AWGN	Additive White Gaussian Noise
BW	Bandwidth
BS	Base Station
DCF	Dropping Coefficient Factor
D2D	Device-to-Device
EE	Energy Efficiency
GPC	Generalized Power Control
IoT	Internet of Things
IUI	Inter-User Interference
LEN	Length
LMMSE	Linear Minimum Mean Square Error
MR	Maximum Ratio
MIMO	Multiple-Input Multiple-Output
PA	Power Amplifier
REF	Reference
RS	Reference Signal
RX	Receiver
SE	Spectral Efficiency
SINR	Signal-to-Interference plus Noise Ratio
SNR	Signal-to-Noise Ratio
SPC	Scaled Power Control
TP	Throughput
TDD	Time Division Duplex
TX	Transmitter

UE	User Equipment
UL	Uplink
ZF	Zero Forcing

References

1. Xu, L.D.; He, W.; Li, S. Internet of Things in Industries: A Survey. *IEEE Trans. Ind. Informat* **2014**, *10*, 2233–2243. [CrossRef]
2. Mu, Y.; Garg, N.; Ratnarajah, T. Federated Learning in Massive MIMO 6G Networks: Convergence Analysis and Communication-Efficient Design. *IEEE Trans. Netw. Sci. Eng.* **2022**, *early access*. [CrossRef]
3. Lee, B.M.; Yang, H. Massive MIMO with Massive Connectivity for Industrial Internet of Things. *IEEE Trans. Ind. Electron.* **2020**, *67*, 5187–5196. [CrossRef]
4. Ciuonzo, D.; Rossi, P.S.; Dey, S. Massive MIMO channel-aware decision fusion. *IEEE Trans. Signal Process.* **2015**, *63*, 604–619. [CrossRef]
5. Shirazinia, A.; Dey, S.; Ciuonzo, D.; Rossi, P.S. Massive MIMO for Decentralized Estimation of a Correlated Source. *IEEE Trans. Signal Process.* **2016**, *64*, 2499–2512. [CrossRef]
6. Lee, B.M.; Yang, H. Energy efficient scheduling and power control of massive MIMO in massive IoT networks. *Expert Syst. Appl.* **2022**, *200*, 116920. [CrossRef]
7. Dey, I.; Ciuonzo, D.; Rossi, P.S. Wideband Collaborative Spectrum Sensing Using Massive MIMO Decision Fusion. *IEEE Trans. Wireless Commun.* **2020**, *19*, 5246–5260. [CrossRef]
8. Zhao, F.; Zhao, L.; Wang, L.; Song, H. An ensemble discrete differential evolution for the distributed blocking flowshop scheduling with minimizing makespan criterion. *Expert Syst. Appl.* **2020**, *160*, 113678. [CrossRef]
9. Zhou, S.; Xing, L.; Zheng, X.; Du, N.; Wang, L.; Zhang, Q. A Self-Adaptive Differential Evolution Algorithm for Scheduling a Single Batch-Processing Machine with Arbitrary Job Sizes and Release Times. *IEEE Trans. Cybern.* **2021**, *51*, 1430–1442. [CrossRef] [PubMed]
10. Zhao, F.; Ma, R.; Wang, L. A Self-Learning Discrete Jaya Algorithm for Multiobjective Energy-Efficient Distributed No-Idle Flow-Shop Scheduling Problem in Heterogeneous Factory System. *IEEE Trans. Cybern.* **2021**, *52*, 12675–12686. [CrossRef]
11. Zhao, F.; He, X.; Wang, L. A Two-Stage Cooperative Evolutionary Algorithm with Problem-Specific Knowledge for Energy-Efficient Scheduling of No-Wait Flow-Shop Problem. *IEEE Trans. Cybern.* **2021**, *51*, 5291–5303. [CrossRef]
12. Zhao, F.; Di, S.; Wang, L. A Hyperheuristic with Q-Learning for the Multiobjective Energy-Efficient Distributed Blocking Flow Shop Scheduling Problem. *IEEE Trans. Cybern.* **2022**, *53*, 3337–3350. [CrossRef]
13. Zhao, F.; Xu, Z.; Wang, L.; Zhu, N.; Xu, T.; Jonrinaldi, J. A Population-Based Iterated Greedy Algorithm for Distributed Assembly No-Wait Flow-Shop Scheduling Problem. *IEEE Trans Industr. Inform.* **2022**, *19*, 6692–6705. [CrossRef]
14. Fitzgerald, E.; Pioro, M.; Tufvesson, F. Massive MIMO Optimization with Compatible Sets. *IEEE Trans. Wireless Commun.* **2019**, *18*, 2794–2812. [CrossRef]
15. Xu, H.; Xu, W.; Yang, Z.; Shi, J.; Chen, M. Pilot Reuse Among D2D Users in D2D Underlaid Massive MIMO Systems. *IEEE Trans. Veh. Technol.* **2018**, *67*, 467–482. [CrossRef]
16. Bai, T.; Heath, R.W., Jr. Analyzing Uplink SINR and Rate in Massive MIMO Systems Using Stochastic Geometry. *IEEE Trans. Commun.* **2016**, *64*, 4592–4606. [CrossRef]
17. Bjornson, E.; Larsson, E.G.; Debbah, M. Massive MIMO for Maximal Spectral Efficiency: How Many Users and Pilots Should Be Allocated? *IEEE Wirel. Commun.* **2016**, *15*, 1293–1308. [CrossRef]
18. Yang, H.; Marzetta, T.L. Massive MIMO with Max-Min Power Control in Line-of-Sight Propagation Environment. *IEEE Trans. Commun.* **2017**, *65*, 4685–4693. [CrossRef]
19. Farsaei, A.; Alvarado, A.; Willems, F.M.J.; Gustavsson, U. An Improved Dropping Algorithm for Line-of-Sight Massive MIMO with Tomlinson-Harashima Precoding. *IEEE Commun. Lett.* **2019**, *23*, 2099–2103. [CrossRef]
20. Marzetta, T.L.; Larsson, E.G.; Yang, H.; Ngo, H.Q. *Fundamentals of Massive MIMO*; Cambridge University Press: London, UK, 2016.
21. Lee, B.M. Adaptive Switching Scheme for RS Overhead Reduction in Massive MIMO with Industrial Internet of Things. *IEEE Internet Things J.* **2021**, *8*, 2585–2602. [CrossRef]
22. Bjornson, E.; Sanguinetti, L.; Hoydis, J.; Debbah, M. Optimal Design of Energy-Efficient Multi-User MIMO Systems: Is Massive MIMO the Answer? *IEEE Trans. Wireless Commun.* **2015**, *14*, 3059–3075. [CrossRef]
23. Jain, R.; Chiu, D.M.; Hawe, W. *A Quantitative Measure of Fairness and Discrimination for Resource Allocation in Shared Computer Systems*; DEC Research Report TR-301; Digital Equipment Corporation: Hudson, MA, USA, 1984.
24. Lee, B.M.; Yang, H. Energy Efficient Massive MIMO in Massive Industrial Internet of Things Networks. *IEEE Internet Things J.* **2022**, *9*, 3657–3671. [CrossRef]
25. ETSI. *Technical Report 136.931 Radio Frequency (RF) Requirements for LTE Pico Node B*; European Telecommunications Standards Institute: Sophia Antipolis, France, 2012.